[Frontiers in Bioscience 12, 1680-1690, January 1, 2007]

Craniofacial, skeletal, and cardiac defects associated with altered embryonic murine *Zic3* expression following targeted insertion of a PGK-NEO cassette

Lirong Zhu [1], Jian Lan Peng [1], Karine G. Harutyunyan [1], Monica D. Garcia [2], Monica J. Justice [1], and John W. Belmont [1]

Departments of [1] Molecular and Human Genetics, and [2] Molecular Physiology and Biophysics, Baylor College of Medicine, One Baylor Plaza, Houston, TX 77030

TABLE OF CONTENTS

1. ABSTRACT

Mutation in *ZIC3* (OMIM #306955), a zinc finger transcription factor, causes heterotaxy (situs ambiguus) or isolated congenital heart defects in humans. Mice bearing a null mutation in *Zic3* have left-right patterning defects with associated cardiovascular, vertebra/rib, and central nervous system malformations. Although *XZic3* is thought to play a critical role in *Xenopus* neural crest development, no defects in tissues derived from neural crest are apparent in adult *Zic3^{null}* mice. In this study we have characterized the effect of a PGK-neo cassette insertion 5' of the *Zic3* locus. The *Zic3* transcript in this new allele is up-regulated in ES cells and in E9.0 embryos, but no ectopic expression was detected. Unlike the *Zic3^{null}* mutation in which only 20% of mutant animals survive to adulthood, there was no evidence of excess fetal death caused by the *Zic3^{neo}* allele. *Zic3^{neo}* mutant mice exhibited hemifacial microsomia, asymmetric low set ears, axial skeletal defects, kyphosis and scoliosis; a combination of defects which mimics Goldenhar Syndrome. Some *Zic3^{neo}* mice had evidence of left-right axis patterning defects, but cardiac malformation was much less common than in the *Zic3^{null}* mutants. A six-week old hemizygous mouse was found to have thoraco-cervical ectopia cordis, an extremely rare congenital malformation in humans and for which there is no precedent in a mouse model.

2. INTRODUCTION

Zic3 is an X chromosome encoded member of the Zic family of transcription factors. There are four other members of the *Zic* gene family, each of which shares five highly conserved C2H2-type zinc finger motifs (1-3). The Zic genes belong to the GLI transcription factor superfamily based on their similarity to the zinc-finger motifs found in GLI proteins (GLI1, GLI2, and GLI3). The *Drosophila* homologue of *GLI*/*Zic* genes, the pair-rule gene *odd-paired (opa)*, is critical for the development of visceral mesoderm, midgut morphogenesis and the establishment of alternate parasegments in the *Drosophila* embryo (4, 5). Murine *Zic3* is expressed in a temporally and spatially restricted pattern in multiple tissues during development. Expression in embryonic mesoderm and ectoderm, dorsal neural tube, dorsomedial somites, neural retina, tail buds, limb buds, and developing brain, imply that it plays roles in multiple developmental processes (6-8). Zic3 deficient mice produced by targeted mutation exhibit complex congenital heart defects, pulmonary reversal or isomerism, central nervous system defects and vertebral/rib anomalies. Embryonic and neonatal lethality is observed in approximately 80% of *Zic3^{null}* mice on the 129/B6 mixed background and no viable *Zic3^{null}* mice on the 129/SvEv inbred background have been observed (9).

ZIC3 was the first gene unequivocally identified as causing human heterotaxy (X-linked heterotaxy, HTX1) (10), a genetically heterogeneous group of congenital disorders resulting from failure to establish normal left-right asymmetry during embryonic development. To date, there have been five missense mutations, five nonsense mutations and one frameshift mutation identified in patients with HTX1 or isolated congenital heart defects (10-12). ZIC3 binds specifically to the GLI-consensus DNA binding site, and can activate a wide range of promoters as a transcriptional coactivator (13). Most of the previously detected mutants in *ZIC3* abolish DNA binding *in vitro* and exhibit decreased transcriptional coactivator activity with GLI3 in reporter gene assays (in preparation). A single missense mutation, P217A, maintains DNA binding (unpublished data) and significantly increases reporter gene transactivation. It is of interest that the patient with P217A mutation did not have heterotaxy (evidence of disrupted left-right patterning in at least one organ system) but rather had an isolated congenital heart defect involving the pulmonary valve (12).

Neural crest cells are a group of ecto-mesenchymal cells that originate from the dorsal aspect of the neural tube, delaminate and migrate along defined pathways to populate numerous structures throughout the embryo. Cranial neural crest derives from the anterior neural tube (forebrain, midbrain and hindbrain), migrates, proliferates and eventually differentiates into cartilage, bone and connective tissues in the head and neck region (14). Cardiac neural crest is a specific cell population responsible for the formation and reorganization of the outflow tract of the developing heart and contributes to the smooth muscle of arch arteries (15). Zic3 is expressed in the neural folds including the neural crest in *Xenopus* and overexpression of *XZic3* in *Xenopus* embryo induced expression of all the neural crest marker genes (16). Overexpression of other *Zic* genes (*XZic1*, *XZic2*, *and XZic5*) also resulted in neural crest formation (17, 18). In mice, all the *Zic* genes (*Zic1-5*) are expressed in the dorsal neural tube (2, 8, 19). A hypomorphic mutation in *Zic2* caused impaired formation of dorsal root ganglion, a neural crest derived tissue (20). The *Kumba* (*Ku*) mutant allele, in which a missense mutation was induced in the fourth zinc finger domain of *Zic2* by ENU mutagenesis, had delayed neural crest production and generated fewer neural crest cells at all axial levels (21). A recent study shows that Zic5-deficient mice exhibited malformation of neural-crest-derived facial bones, especially the mandible (2). However, there is no description of abnormal neural-crest-derived tissues in $Zic3^{null}$ mice (9) or in *bent tail* mice which have a deletion encompassing the Zic3 locus (7, 22-24). The role of Zic3 in mouse neural crest development is, therefore, uncertain.

In this study, we examined a Zic3 allele altered by the insertion of a PGK-neo cassette into its proximal upstream region. This appears to cause a reproducible increase in Zic3 transcription but not an altered pattern of expression. Mice bearing this allele showed axial skeleton defects, congenital heart defects, and abnormalities of neural crest derivatives, including zygomatic bone, mandible, hyoid bone and laryngeal cartilage. Our results indicate that Zic3 plays multiple roles in normal organogenesis and the balance of *Zic* family expression may have specific effects on murine neural crest development.

3. MATERIALS AND METHODS

3.1. Generation of the targeting vector

The RPCI-22 mouse female (129S6/SvEvTac) mouse bacterial artificial chromosome (BAC) genomic library (BACPAC Resources Center at Children's Hospital Oakland Research Institute in Oakland, CA) was screened by two 36bp overgo probes located in Zic3 exon 1, and seven positive BAC clones were identified and further confirmed by both PCR and enzyme digestion. The plasmid DNA was isolated from BAC clones by Big BAC DNA isolation Kit (Princeton Separations, Inc). An 11.3kb BglII-SpeI fragment containing all the Zic3 exons and introns was isolated from enzyme digestion of the identified BAC plasmids. A 2.2kb SacI-NgoMI fragment (containing the 5' flanking sequence) was placed upstream of the FRT flanking PGK-neo cassette and downstream of the MC1tkpA herpes simplex virus thymidine kinase expression cassette (both cassettes were kindly provided by Dr. James F. Martin, Alkek Institute of Biosciences and Technology, Texas A&M System Health Science Center). A 2.1kb NgoMI-AfeI fragment (containing Zic3 exon 1) was inserted downstream of the FRT flanking PGK-neo cassette. The targeting vector was linearized at a unique PmeI site outside the region of sequence homology.

3.2. Electroporation, selection and screening of embryonic stem (ES) cells

The linearized targeting vector was electroporated into AB2.2 ES cells which is at passage 18. Following electroporation, cells were cultured on tissue culture plates containing mitomycin C-treated fibroblast feeder layers. After 24h, the media was replaced with selection media containing, in addition to routine supplements, G418 and FIAU. After 8 days selection, individual G418/FIAU-resistant ES cell clones were screened by BstXI digestion and hybridized with a unique 5' probe external to the region of vector homology.

3.3. Blastocyst injection and animal breeding

ES cells from two positive clones were trypsinized, centrifuged, and resuspended in injection media. ES cells were microinjected into blastocyst-stage embryos derived from C57BL/6J albino female mice. Cultured embryos were implanted into the uterus of pseudopregnant ICR mice. High-level male chimeras were bred with wild-type C57BL/6J albino females to obtain germ line transmission offspring. Since the transgene is located in X chromosome, all the female offspring with germ line transmission are heterozygotes for the $Zic3^{neo}$ allele, while all the male offspring are wildtype. $Zic3^{neo}$ heterozygotes were mated with wildtype C57BL/6J albino males to get $Zic3^{neo}$ hemizygotes and heterozygotes. Meanwhile, $Zic3^{neo}$ heterozygotes were backcrossed to chimeras with high percentage of germ line transmission to obtain $Zic3^{neo}$ homozygotes. The structure of the modified *Zic3* locus was characterized by extensive Southern blot (5' locus-specific probes), PCR analysis (sites flanking the expected boundaries of the neo cassette insertion) and DNA

sequencing of the direct PCR products. In order to derive inbred mutant mice on a 129S6/SvEv background, chimeras were mated with 129S6/SvEv inbred female mice (purchased from Taconic, NY). Offspring were genotyped by PCR to validate the expected transmission of the *Zic3*^{neo} allele and these heterozygotes were further mated to 129S6/SvEv males.

3.4. Isolation of RNA, quantitative PCR and whole-mount *in situ* hybridization

Mice were maintained on a 0600 to 2000 hours light-dark cycle, with noon of the day of observation of a vaginal plug defined as E0.5. Mouse embryos were harvested at E9.0. RNeasy Mini Kit (QIAGEN) was used to extract RNA from pooled mouse embryos and ES cells and cDNA was synthesized from total RNA using the SuperScript First-Strand synthesis system for RT-PCR (Invitrogen). All primers were optimized on the ABI 7000 SDS using SYBR Green dye incorporation. The following cycling parameters were used for quantitative PCR using ABI 7000 SDS: 95°C for 10 min, 40 cycles of 95°C for 15 s, and 60°C for 1 min. Expression of Zic3 was compared to an endogenous RNA control, glyceraldehyde-3-phosphate dehydrogenase (GAPDH). The following PCR primers were used: Zic3 F:cgaaggctgtgacagacggt R:catgtgcttcttgcggtcg; GAPDH F:tgtgtccgtcgtggatctga R:cctgcttcaccaccttcttga. Whole-mount *in situ* hybridization was performed using the same protocol described (9). An antisense probe spanning 470 bp in the 3' UTR (position 2825-3295 in NM_009575) of the *Zic3* cDNA was generated by PCR. Probes were labeled using a DIG RNA Labeling kit (Roche).

3.5. Skeletal X-rays and staining

Adult mice were anesthetized by intraperitoneal injection of Avertin (2.5 % working solution) (ml) at a dose of 2% of body weight (g). Mice were imaged on a digital Faxitron MX-20 (Faxitron X-ray Corporation, Wheeling, IL). X-ray exposures were taken at 35 kV for 5 seconds and images were sharpened using the ROI contrast function.

Specific bone and cartilage staining of adult mice was performed according to the previously described procedures (25). In brief, the mice without skin and viscera were fixed in 95% ethanol for 72 hours. Staining of cartilage was performed with 0.05% Alcian blue 8GX (Sigma) 95% ethanol and 20% acetic acid for 48 hours. After re-fixing in 95% ethanol for 2 days, samples were cleared in 2% KOH for 72 hours. Staining of bones was performed in 0.015% of Alizarin red (Sigma) in 1% KOH for 48 hours. The stained skeleton was further cleared in 1% KOH and 20% glycerol and stored in 1:1 mixture of glycerol and 95% ethanol.

4. RESULTS

4.1. Generation of *Zic3*^{neo} allele

As part of a project to analyze the functions of *Zic3* through targeted transgenic modification, a *neo* minigene cassette flanked by FRT sites was inserted in antisense orientation 5' of the first exon of the mouse *Zic3* gene (Figure 1A). The FRT sites were included to permit *in vivo* deletion of the cassette. The linearized targeting construct was electroporated into AB2.2 ES cells and, after G418 and FIAU selection, resistant clones were screened by Southern blot of BstXI-digested genomic DNA (Figure 1B). Eighteen clones showed evidence of homologous recombination within the *Zic3* locus from 192 clones tested. Five of these recombinant ES cell clones were chosen for expansion. Two ES cell clones were used for injection into the blastocysts of C57BL/6J albino female mice. Four male chimeras were chosen for mating with C57BL/6J albino female mice. All offspring of two male chimeras had agouti fur color, consistent with a germline in those chimeras composed mostly of the daughter cells of the targeted ES cells and essentially complete transmission of the X chromosome targeted *Zic3* allele to all female N1 progeny. Because *Zic3* is X linked, all the N1 males are wild-type. Heterozygous females were backcrossed to these same 2 chimeras to obtain homozygous and hemizygous *Zic3*^{neo} mice. The presence of *Zic3*^{neo} allele in mutant mice was confirmed by both PCR and Southern blot analysis (Figure 1C, D).

4.2. *Zic3* mRNA was over-expressed from the *Zic3*^{neo} allele

Zic3 is expressed in the embryonic epiblast and in cultured ES cells. In order to determine whether the PGK-neo cassette altered *Zic3* expression, RNA was isolated from *Zic3*^{neo}/*y* and wildtype parental ES cells (129S6/SvEv derived). Quantitative realtime PCR was used to detect the *Zic3* mRNA levels using a pair of primers located in exon 2. As shown in Figure 2a, the expression level of *Zic3* in *Zic3*^{neo}/*y* ES cells was increased by 1.3-fold compared to that in wildtype ES cells. In order to examine whether *Zic3* expression level was also increased during embryonic development, RNA isolated from E9.0 homozygous and hemizygous *Zic3*^{neo} embryos and E9.0 wildtype embryos was also compared using the same technique. These embryos all are derived from crosses giving a mixed B6/129 background. The *Zic3* expression level in homozygous and hemizygous *Zic3*^{neo} embryos was 1.8-fold higher than the wildype embryos (Figure 2a), confirming that the *Zic3* expression level was also up-regulated at E9.0 by insertion of PGK-neo cassette into *Zic3* locus. *In situ* hybridization was performed in E10.5 homozygous and hemizygous *Zic3*^{neo} embryos and E10.5 wildtype embryos using an antisense *Zic3* riboprobe to analyze *Zic3* mRNA expression. No ectopic expression of *Zic3* in *Zic3*^{neo} allele was detected, compared to the wildtype allele (Figure 2b,c).

4.3. No embryonic lethality observed in mice bearing the *Zic3*^{neo} allele

Complete *Zic3* deficiency causes both embryonic and postnatal lethality, the penetrance of which is sensitive to genetic background differences (9). In order to investigate whether up-regulation of *Zic3* could also lead to embryonic lethality, heterozygous *Zic3*^{neo}/+ mice derived from crosses of male chimeras with C57BL/6J albino mice were bred with *Zic3*^{neo}/*y* males. Their progeny (n=111) were genotyped at P21. The results (Table 1) indicate that

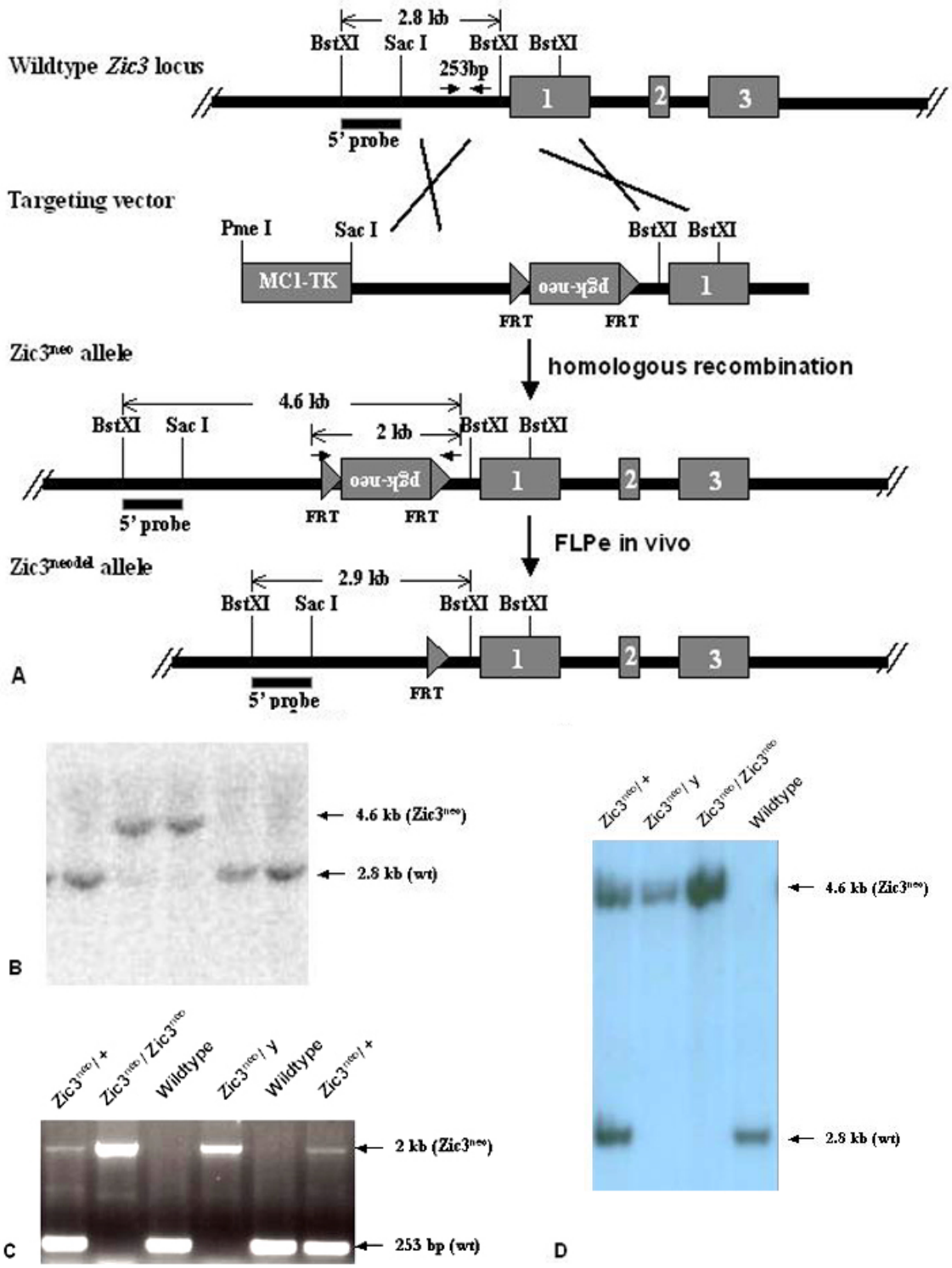

Figure 1. Generation of the Zic3^{neo} allele. A. A PGK-neo cassette was inserted in antisense orientation 5' of the first exon of the mouse *Zic3* gene by homologous recombination. A 400bp BstXI-SacI fragment external to the region of vector homology was used as a 5'-probe to detect the occurrence of homologous recombination. B. Homologous recombinants were identified by Southern. Genomic DNAs from ES cell clones were digested with BstXI and hybridized with the 5' external probe, detecting a wildtype 2.8kb fragment or a targeted 4.6kb fragment. C. PCR of tail genomic DNA using PCR primers flanking the expected boundaries of the PGK-neo cassette for genotyping progeny. The wildtype allele generates a 253bp product, and the *Zic3^{neo}* allele a 2kb product. D. Genotyping progeny by Southern. Genomic DNAs digested with BstXI and hybridized with the same 5' external probe.

Table 1. No embryonic lethality was observed in *Zic3*^{neo} mice

Mating Strategy	Total Number	Genotypes Analysis at P21				Exact χ^2	P Value
Zic3^{neo}/+ X *Zic3*^{neo}/y		*Zic3*^{neo}/y	+/y	*Zic3*^{neo}/*Zic3*^{neo}	*Zic3*^{neo}/+		
	111	21	30	29	31	2.261	NS
Zic3^{neo}/+ X +/y		*Zic3*^{neo}/y	+/y	*Zic3*^{neo}/+	+/+		
	27	6	7	6	8	.407	NS

Zic3^{neo}/+ was mated with *Zic3*^{neo}/y and 111 P21 offspring were genotyped. A chi-square exact test (df=3, performed in SPSS 11.0) showed there was no significant departure from the expected Mendelian ratios. *Zic3*^{neo}/+ was also mated with +/y and 27 of their offspring at P21 were genotyped. There was no significant departure from the expected Mendelian ratios. NS -not significant.

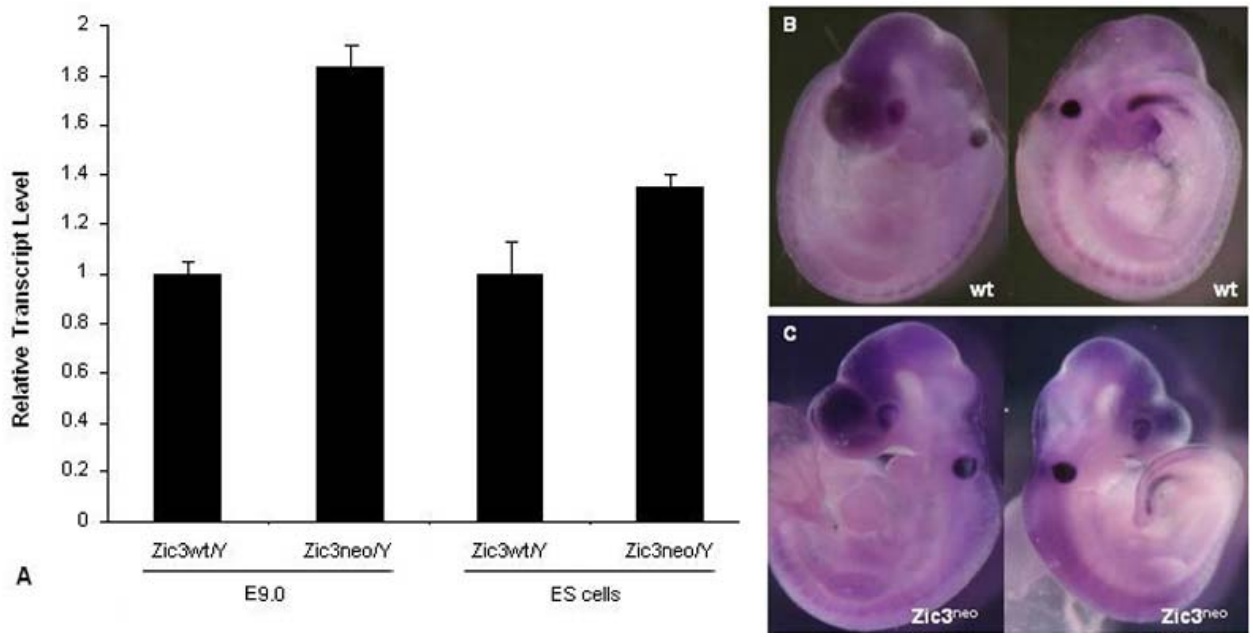

Figure 2. *Zic3* mRNA was over-expressed in *Zic3*^{neo} embryos and ES cells. A. RNA was extracted and cDNA synthesized by reverse transcription. Quantitative PCR was performed to detect the *Zic3* expression level using a pair of primers located in exon 2. The results were normalized by reference to an endogenous RNA GAPDH control. B, C. Whole mount *in situ* hybridization with antisense *Zic3* probe on E10.5 wildtype and *Zic3*^{neo} embryos.

there is no significant departure from the expected Mendelian ratios. Male chimeras were also mated with 129S6/SvEv wildtype females to obtain the *Zic3*^{neo}/+ females and these mice were then mated with 129S6/SvEv wildtype males. Genotyping of their progeny at P21 also showed that the percentage of each genotype fit the expected ratios. Since the PGK-neo cassette is flanked by FRT sites, we mated mice with the *Zic3*^{neo} allele with FLPeR mice (26) (purchased from the Jackson Laboratory) to delete the PGK-neo cassette (designed by *Zic3*^{neodel}) by FLPe-FRT recombination. Necropsy and skeleton preparation study on twenty homozygous and hemizygous *Zic3*^{neodel} mice did not reveal any abnormalities (data not shown), indicating that the abnormalities identified in *Zic3*^{neo} mice (described below) resulted from the insertion of PGK-neo.

4.4. Left-right axis abnormalities and axial skeletal defects in mice bearing the *Zic3*^{neo} allele

Zic3 deficiency in both mice and humans often leads to left right patterning defects. To investigate whether altered expression of Zic3 caused by the insertion in the *Zic3*^{neo} could also lead to left-right patterning defects, thirty-eight homozygous and hemizygous *Zic3*^{neo} 4-week-old adults were analyzed. Dextrocardia was identified in 7.9%. One homozygous female had left-sided gall bladder and one hemizygous male had asplenia. The position, number and size of spleen were normal in the remainder. In addition, fifty-eight homozygous and hemizygous *Zic3*^{neo} embryos were analyzed at E14.5-15.5 to examine the left-right axis of thoracic cavity and the cardiac great vessels. Four of them (6.9%) were found to have dextrocardia. However, unlike the *Zic3*^{null} mutants, no dextro-transposition of the great arteries, interrupted aortic arch and right aortic arch was observed. No pulmonary isomerism or complete left-right reversal of the lung lobes was identified in any adult or embryo.

All *Zic3*^{null}/*y* mice, high level male chimeras and >40% of *Zic3*^{null}/+ females have "kinked" tails. This malformation results from distal vertebral body anomalies and is associated with other disturbances in axial skeleton and neural tube development. Vertebral anomalies of the tail were found, albeit less frequently, in animals bearing the *Zic3*^{neo} allele. Sixty homozygous and hemizygous *Zic3*^{neo} mice were examined and five (8.3%) had tail kinks

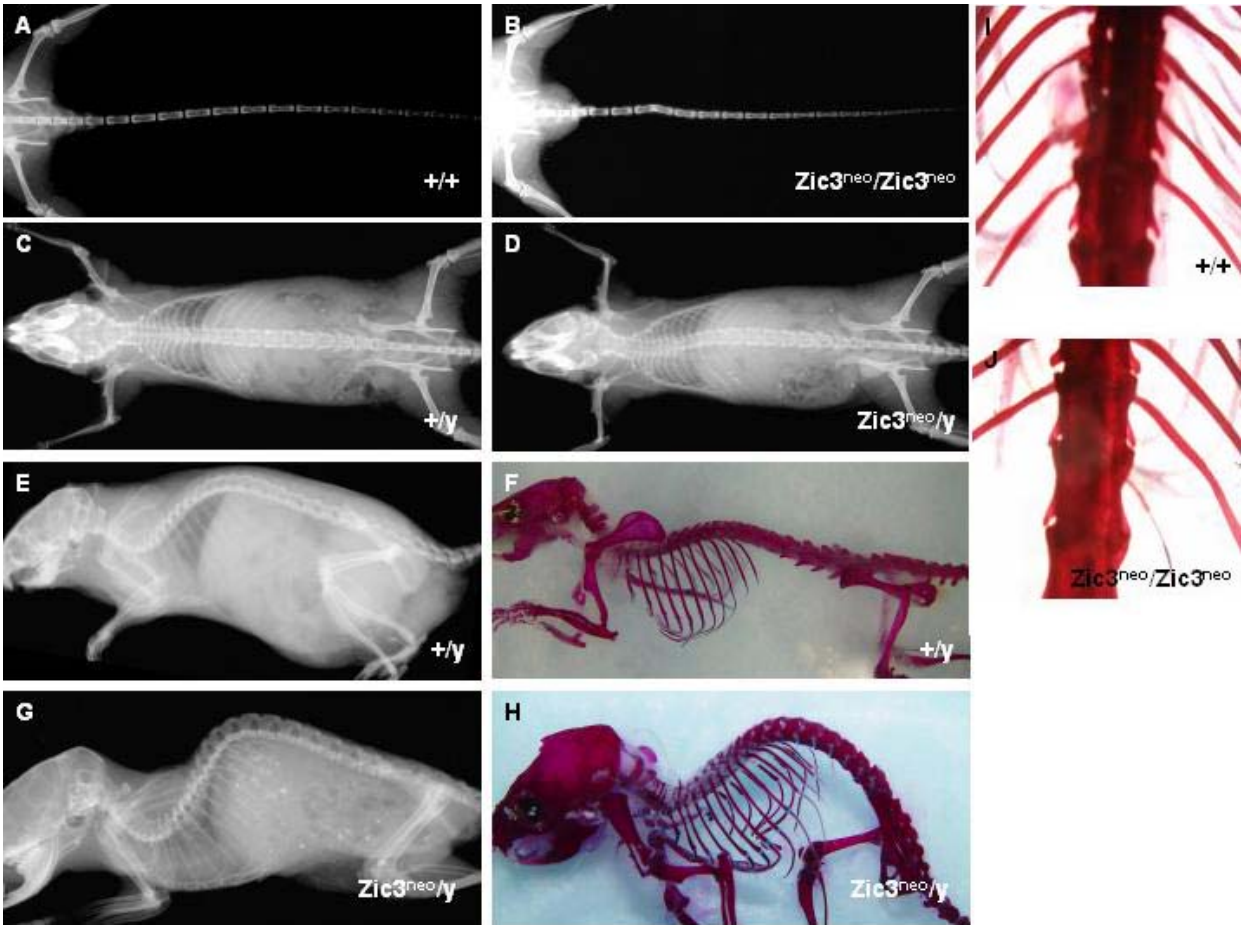

Figure 3. Axial skeletal defects in mice bearing the *Zic3*^{neo} allele. Skeletal X-rays of wild type (A, C, E) and *Zic3*^{neo} mice (B, D, G). Note the kinked tail (B) and thoracolumbar scoliosis (D) or kyphosis (G). Skeleton preparation of wild type (F,I) and *Zic3*^{neo} mice (H,J). Thoracolumbar kyphosis (H) and Lack of the left 13th rib (J).

(Figure 3B). "Kinked" tails in other mouse models are often associated with more severe neural tube defects, including spina bifida, meningocoele and exencephaly (23). In order to determine whether neural tube defects developed in *Zic3*^{neo} allele, thirty-nine E10.5, twenty-one E12.5, and fifty-eight E14.5-15.5 homozygous and hemizygous *Zic3*^{neo} embryos were examined, however no exencephaly or other open neural tube malformations were observed.

A high percentage of adult *Zic3*^{neo} animals exhibited obvious progressive spine defects. Skeletal survey by X-ray of forty-eight homozygous and hemizygous two-month-old *Zic3*^{neo} adults revealed twenty-two (45.8%) developed thoracolumbar kyphosis and an additional seven (14.6%) developed thoracolumbar scoliosis (Figure 3D). Further skeleton preparation using Alcian blue/Alizarin red staining confirmed the existence of kyphosis (Figure 3H), but no vertebral body defects were found. One homozygote was found lacking the left 13th rib (Figure 3J). The mechanism of kyphoscoliosis is unclear from these studies but does not appear to be due to a primary disorder of bone development.

4.5. Craniofacial anomalies, hyoid bone and cricoid cartilage defects in *Zic3*^{neo} mice

Growth retardation was found in eight out of ninety (8.9%) homozygous and hemizygous Zic3^{neo} mice at weaning age. Further study of the mice with growth retardation revealed that they had severe malocclusion (Figure 4A, B). These animals typically died within two months from insufficient feeding. Mice with malocclusion had prominent abnormal facial phenotypes, including hemifacial microsomia, asymmetric low set ears (Figure 4C, F, G), deviation of the mandible from the midline, and unilateral hypertrophy of the mandibular musculature (Figure 4D). Skeleton preparations were used to evaluate for craniofacial bone anomalies. The abnormalities include asymmetric distance between the external auditory meatus and the orbital fossa (Figure 4F, G), hypoplasia of the maxilla and premaxilla leading to asymmetric position of the zygomatic bone (Figure 4H, I), and unilateral underdevelopment of coronoid process of mandible (Figure 4J). The squamosal portion of the temporal bone and the frontal bone appear relatively spared. All the mice with malocclusion were also found to have kyphosis.

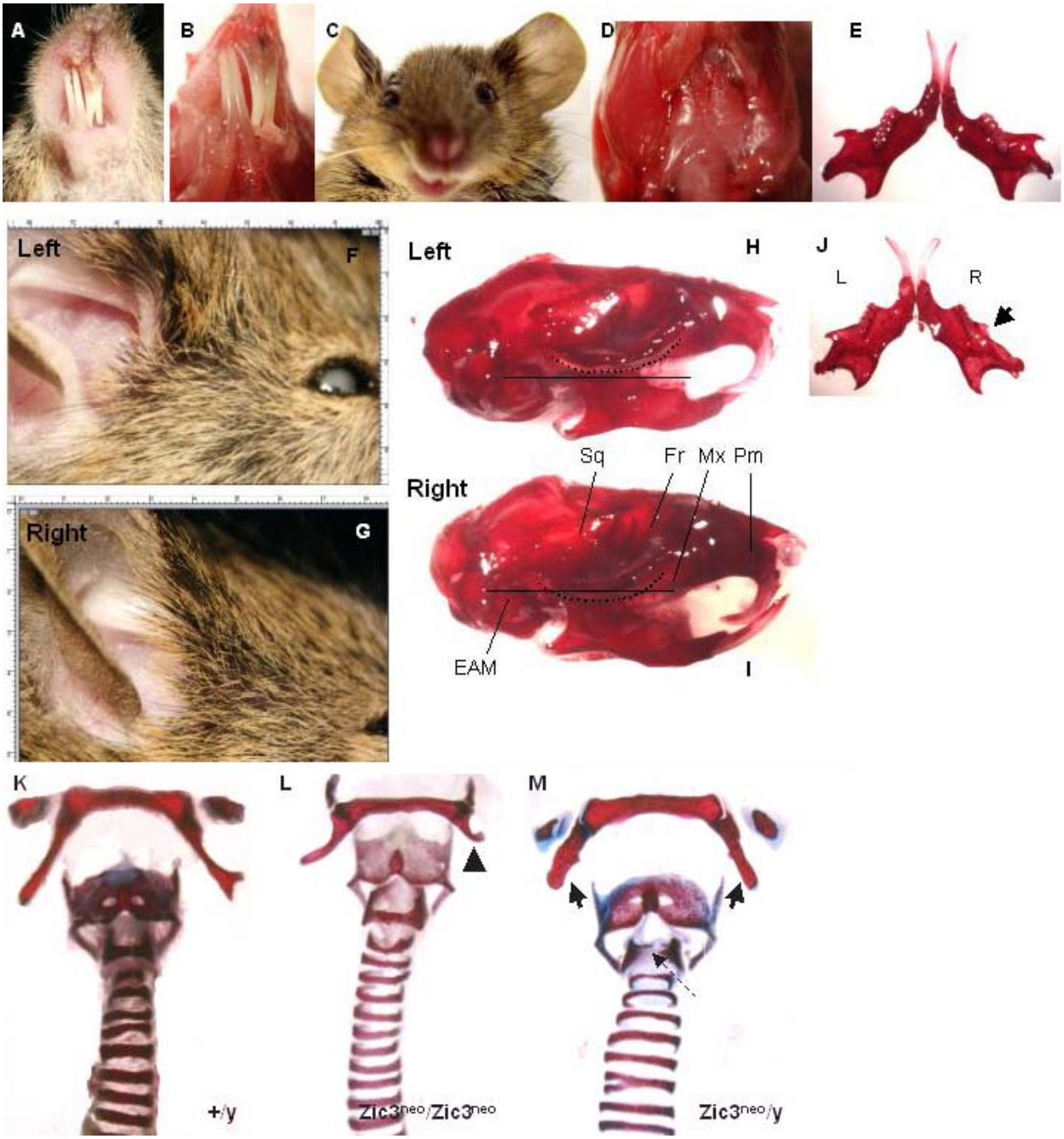

Figure 4. Malocclusion, craniofacial anomalies**,** hyoid bone and cricoid cartilage defects identified in *Zic3*^{neo} mice. A, B. Malocclusion observed by necropsy. C. Hemifacial microsomia (frontal view). Note the asymmetric low set ears. D. Asymmetric hypertrophy of mandibular musculature (arrow). E. Symmetric size of the body and ramus of the mandible. F,G. Hemifacial microsomia. Note the dysplastic left ear, the decreased distance from and inferior displacement of the left external auditory canal relative to the palpebral fissure, as well as the left congenital cataract. H,I Lateral views of skull: demonstrates asymmetric superior displacement of the zygomatic (dotted curve) relative to the rostral boundary of the external auditory meatus (EAM, marked by solid line) with accompanying hypoplasia of the maxilla (Mx) and premaxilla (Pm) and relative sparing of the frontal (Fr) and squamosal (Sq) bones. J. Underdevelopment of coronoid process of mandible on the right side (indicated by arrow). K. Normal hyoid bone and laryngeal cartilage observed in wildtype mouse by skeleton preparation. L. Note the aplasia of the left greater horn of the hyoid bone (indicated by arrowbar). M. Abnormal shape of the greater horns of the hyoid bone and failure of fusion of cricoid bone in the midline (indicated by arrows).

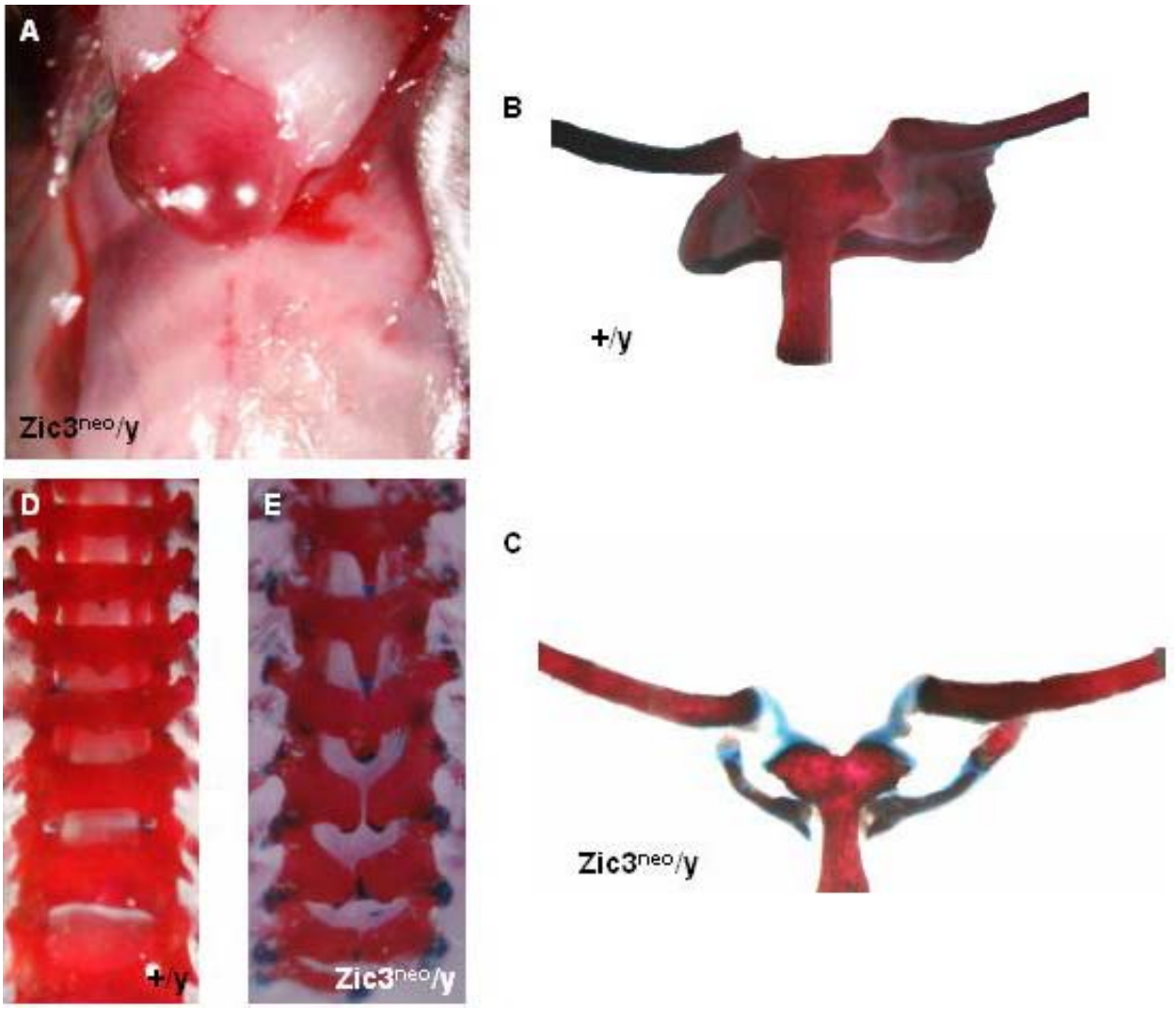

Figure 5. Ectopia cordis in *Zic3*^{neo} mouse. A. Thoraco-cervical ectopia cordis found during necropsy. Note that there is no defect in thoracic wall and the heart is located in the midline. C. Skeleton preparation revealed the split in upper portion of the sternal manubrium, compared to the wildtype shown in B. E. Note the failure of fusion of the lamina leading to open vertebral foramen in T10-12, compared to the wildtype shown in D.

In addition to craniofacial defects, the homozygous and hemizygous Zic3^{neo} mutants exhibited defects in hyoid bone and cricoid cartilage (Figure 4K, L, M). Those abnormalities include asymmetric length and shape of hyoid bone, and failure of fusion of cricoid cartilage in the midline.

4.6. Ectopia cordis

Ectopia cordis is a very rare congenital malformation in which the heart is located partially or totally outside of the thoracic cavity. It occurs in 5.5 to 7.9 per 1 million live births (27). We examined a six-week-old *Zic3*^{neo} /y mouse and unexpectedly found it had ectopia cordis at necropsy (Figure 5A). The mouse was active and appeared healthy before anesthesia. It was indistinguishable from wildtype littermates in length and body weight and there was no abnormality of the ventral skin. The heart was located in the midline between the dermis and the thoracic cavity. The rostral boundary of the heart was at the level of 5th cervical vertebra i.e. significant anterior displacement compared to normal. Examination of the cardiac great vessels showed that the right common carotid artery and the right subclavian artery derive from the aortic artery directly, and the brachiocephalic artery was absent. The lungs were hypoplastic and located in a relative midline position of the thoracic cavity, but the lobation was normal. Skeleton preparation study revealed a split in upper portion of the sternal manubrium and failure of fusion of neural arches of T10-12 in the midline (Figure 5C).

5. DISCUSSION

PGK-neo, a hybrid gene consisting of the phosphoglycerate kinase I promoter driving the neomycin phosphotransferase gene, is frequently used as a positive selection marker for gene-targeting in mouse embryonic stem cells. However, the introduction of a PGK-neo cassette

can interfere with endogenous promoters in the targeted locus and affect the expression level of the transcripts (28), since the PGK promoter functions as a strong promoter/enhancer. In the present study, the insertion of PGK-neo cassette in the antisense orientation to *Zic3* led to mild overexpression of the downstream *Zic3* transcript in both ES cells and E9.0 embryos, confirming previous reports that the activity of PGK promoter can be bidirectional (29-31).

Homozygous and hemizygous *Zic3^{neo}* mice developed multiple birth defects, including skeleton/rib abnormalities, craniofacial anomalies, left-right axis defects, congenital heart defects, hyoid bone and laryngeal cartilage abnormalities. Penetrance of the individual defects with the exception of kyphoscoliosis was relatively low, a situation that parallels the familial clustering of similar birth defects in humans. There were no systematic differences seen between *Zic3^{neo}/y* and *Zic3^{neo}/ Zic3^{neo}* in any of these phenotypes.

Zic3^{neo} mice exhibited hemifacial microsomia and asymmetric low set ears. These abnormalities are somewhat similar to those seen in mice bearing mutations in Tbx1 although in those animals the defects are generally symmetric (32). Another mouse model, *Hfm*, produces a similar asymmetric facial and skull phenotype with low penetrance (33, 34). *Hfm* resulted from a transgene insertion/deletion in an evolutionarily conserved region on mouse chromosome 10 (34), but specific gene identification has not yet been reported. The skeleton preparations suggest that unilateral hypertrophy of the jaw was not derived from asymmetric development of the body and ramus of the mandible (Figure 4E). Rather, it seems to have arisen due to unbalanced use of the masticatory muscles secondary to malocclusion. The mobile coronoid process articulates with the glenoid fossa of the temporal bone and forms the temporomandibular joint. Underdevelopment of the coronoid process of mandible can lead to ipsilateral deviation of the mandible from the midline and result in severe malocclusion. The hyoid bone abnormalities found in *Zic3^{neo}* mice include unilateral aplasia of the greater horns, abnormal shape of the greater horn, and abnormal orientation of the lesser horn. The mandible and part of zygomatic bone are the derivatives of the first pharyngeal arch. The lesser horn is derived from the second pharyngeal arch, while the greater horn is from the third pharyngeal arch. The normal development of pharyngeal arches requires essential contributions from neural crest cells (35). Neural crest cells are a population of cells which emerge from the dorsal neural tube region. Previous work has shown that *Zic3* is expressed in the dorsal neural tube region during development and over expression of *XZic3* demonstrates that it plays a critical role in *Xenopus* neural crest development (8, 16). However, no neural crest abnormalities were observed in Zic3 deficient mice. Relatively subtle neural crest defects were found in Zic2 hypomorph and Zic5 deficient mice (2, 21). Given the function of *Xenopus* Zic1, Zic2, Zic3 and Zic5 in neural crest development (16-18), it is very likely that the absence of obvious neural crest defects in Zic3 deficient mice is due to functional redundancy of Zic family genes.

Hemifacial microsomia, asymmetric low set ears, hypoplasia of the mandible and vertebra defects are well-recognized birth defects in humans. They are typical features of Goldenhar Syndrome (also known as oculo-auriculo-vertebral spectrum or First and Second Branchial Arch Syndrome). Goldenhar Syndrome has an estimated birth prevalence of 1:45,000 (36) to 1:10,000 births (37). The mechanisms underlying Goldenhar Syndrome remain unknown. Given the craniofacial phenotype, it is very likely that the altered regulation of neural crest development plays a central role. Patients with Goldenhar Syndrome also often have eye, ear, cardiovascular, and genitourinary defects (38). There are several reports that Goldenhar Syndrome can be associated with left-right patterning defects (39). We speculate that ZIC3 or a ZIC3-regulated pathway could be important in this condition. Screening for *ZIC3* mutations in the patients with Goldenhar Syndrome should be considered.

Ectopia cordis is a rare and striking congenital heart defect first described in 1671 (cited in ref (40)). The defect involves congenital malposition of the heart partially or completely outside the thoracic cavity. To our knowledge ectopia cordis has never been reported in live born mice. Ectopia cordis can be classified into five types (40): 1) cervical, in which the heart is entirely in the cervical region with intact sternum; 2) thoraco-cervical, in which the heart is partially in the cervical region but the cranial end of the sternum is split; 3) thoracic, in which the sternum is completely split or absent, and the heart lies partially or completely outside the thorax; 4) thoraco-abdominal, in which the heart exists in a direct communication between the thoracic and the abdominal cavities and usually accompanies Pentalogy of Cantrell; 5) abdominal, in which the heart passes through a defect in the diaphragm to enter the abdominal cavity. Using this classification, the ectopic cordis found in our *Zic3^{neo}* hemizygote belongs to the category of thoraco-cervical ectopic cordis (only two among 48 cases between 1938-1961). Detailed studies of the skeleton in this mouse revealed midline fusion defects, including split of the upper portion of the sternal manubrium. Interestingly, the heart was located in the midline of the cervical and thoracic region, suggesting that a left-right patterning process might be associated with the development of ectopic cordis.

6. ACKNOWLEGEMENT

We thank Isabel Lorenzo in Darwin Transgenic Core Facility at Baylor College of Medicine for performing Embryonic Stem Cell Culture and Microinjection Services. This work was supported by grants from the National Institutes of Health (HD39056 and HL067155).

7. REFERENCES

1. Aruga, J., T. Nagai, T. Tokuyama, Y. Hayashizaki, Y. Okazaki, V. M. Chapman & K. Mikoshiba: The mouse zic gene family. Homologues of the Drosophila pair-rule gene odd-paired. *J Biol Chem*, 271, 1043-7 (1996)

2. Inoue, T., M. Hatayama, T. Tohmonda, S. Itohara, J. Aruga & K. Mikoshiba: Mouse Zic5 deficiency results in

neural tube defects and hypoplasia of cephalic neural crest derivatives. *Dev Biol*, 270, 146-62 (2004)
3. Aruga, J., N. Yokota, M. Hashimoto, T. Furuichi, M. Fukuda & K. Mikoshiba: A novel zinc finger protein, zic, is involved in neurogenesis, especially in the cell lineage of cerebellar granule cells. *J Neurochem*, 63, 1880-90 (1994)
4. Cimbora, D. M. & S. Sakonju: Drosophila midgut morphogenesis requires the function of the segmentation gene odd-paired. *Dev Biol*, 169, 580-95 (1995)
5. Benedyk, M. J., J. R. Mullen & S. DiNardo: odd-paired: a zinc finger pair-rule protein required for the timely activation of engrailed and wingless in Drosophila embryos. *Genes Dev*, 8, 105-17 (1994)
6. Elms, P., A. Scurry, J. Davies, C. Willoughby, T. Hacker, D. Bogani & R. Arkell: Overlapping and distinct expression domains of Zic2 and Zic3 during mouse gastrulation. *Gene Expr Patterns*, 4, 505-11 (2004)
7. Herman, G. E. & H. M. El-Hodiri: The role of ZIC3 in vertebrate development. *Cytogenet Genome Res*, 99, 229-35 (2002)
8. Nagai, T., J. Aruga, S. Takada, T. Gunther, R. Sporle, K. Schughart & K. Mikoshiba: The expression of the mouse Zic1, Zic2, and Zic3 gene suggests an essential role for Zic genes in body pattern formation. *Dev Biol*, 182, 299-313 (1997)
9. Purandare, S. M., S. M. Ware, K. M. Kwan, M. Gebbia, M. T. Bassi, J. M. Deng, H. Vogel, R. R. Behringer, J. W. Belmont & B. Casey: A complex syndrome of left-right axis, central nervous system and axial skeleton defects in Zic3 mutant mice. *Development*, 129, 2293-302 (2002)
10. Gebbia, M., G. B. Ferrero, G. Pilia, M. T. Bassi, A. Aylsworth, M. Penman-Splitt, L. M. Bird, J. S. Bamforth, J. Burn, D. Schlessinger, D. L. Nelson & B. Casey: X-linked situs abnormalities result from mutations in ZIC3. *Nat Genet*, 17, 305-8 (1997)
11. Megarbane, A., N. Salem, E. Stephan, R. Ashoush, D. Lenoir, V. Delague, R. Kassab, J. Loiselet & P. Bouvagnet: X-linked transposition of the great arteries and incomplete penetrance among males with a nonsense mutation in ZIC3. *Eur J Hum Genet*, 8, 704-8 (2000)
12. Ware, S. M., J. Peng, L. Zhu, S. Fernbach, S. Colicos, B. Casey, J. Towbin & J. W. Belmont: Identification and functional analysis of ZIC3 mutations in heterotaxy and related congenital heart defects. *Am J Hum Genet*, 74, 93-105 (2004)
13. Mizugishi, K., J. Aruga, K. Nakata & K. Mikoshiba: Molecular properties of Zic proteins as transcriptional regulators and their relationship to GLI proteins. *J Biol Chem*, 276, 2180-8 (2001)
14. Chai, Y., X. Jiang, Y. Ito, P. Bringas, Jr., J. Han, D. H. Rowitch, P. Soriano, A. P. McMahon & H. M. Sucov: Fate of the mammalian cranial neural crest during tooth and mandibular morphogenesis. *Development*, 127, 1671-9 (2000)
15. Jiang, X., D. H. Rowitch, P. Soriano, A. P. McMahon & H. M. Sucov: Fate of the mammalian cardiac neural crest. *Development*, 127, 1607-16 (2000)
16. Nakata, K., T. Nagai, J. Aruga & K. Mikoshiba: Xenopus Zic3, a primary regulator both in neural and neural crest development. *Proc Natl Acad Sci U S A*, 94, 11980-5 (1997)
17. Nakata, K., T. Nagai, J. Aruga & K. Mikoshiba: Xenopus Zic family and its role in neural and neural crest development. *Mech Dev*, 75, 43-51 (1998)
18. Nakata, K., Y. Koyabu, J. Aruga & K. Mikoshiba: A novel member of the Xenopus Zic family, Zic5, mediates neural crest development. *Mech Dev*, 99, 83-91 (2000)
19. Gaston-Massuet, C., D. J. Henderson, N. D. Greene & A. J. Copp: Zic4, a zinc-finger transcription factor, is expressed in the developing mouse nervous system. *Dev Dyn*, 233, 1110-5 (2005)
20. Nagai, T., J. Aruga, O. Minowa, T. Sugimoto, Y. Ohno, T. Noda & K. Mikoshiba: Zic2 regulates the kinetics of neurulation. *Proc Natl Acad Sci U S A*, 97, 1618-23 (2000)
21. Elms, P., P. Siggers, D. Napper, A. Greenfield & R. Arkell: Zic2 is required for neural crest formation and hindbrain patterning during mouse development. *Dev Biol*, 264, 391-406 (2003)
22. Franke, B., R. Klootwijk, J. W. Hekking, R. T. de Boer, H. J. ten Donkelaar, E. C. Mariman & H. W. van Straaten: Analysis of the embryonic phenotype of Bent tail, a mouse model for X-linked neural tube defects. *Anat Embryol (Berl)*, 207, 255-62 (2003)
23. Klootwijk, R., B. Franke, C. E. van der Zee, R. T. de Boer, W. Wilms, F. A. Hol & E. C. Mariman: A deletion encompassing Zic3 in bent tail, a mouse model for X-linked neural tube defects. *Hum Mol Genet*, 9, 1615-22 (2000)
24. Carrel, T., S. M. Purandare, W. Harrison, F. Elder, T. Fox, B. Casey & G. E. Herman: The X-linked mouse mutation Bent tail is associated with a deletion of the Zic3 locus. *Hum Mol Genet*, 9, 1937-42 (2000)
25. Bi, W., T. Ohyama, H. Nakamura, J. Yan, J. Visvanathan, M. J. Justice & J. R. Lupski: Inactivation of Rai1 in mice recapitulates phenotypes observed in chromosome engineered mouse models for Smith-Magenis syndrome. *Hum Mol Genet*, 14, 983-95 (2005)
26. Farley, F. W., P. Soriano, L. S. Steffen & S. M. Dymecki: Widespread recombinase expression using FLPeR (flipper) mice. *Genesis*, 28, 106-10 (2000)
27. Hornberger, L. K., S. D. Colan, J. E. Lock, D. L. Wessel & J. E. Mayer, Jr.: Outcome of patients with ectopia cordis and significant intracardiac defects. *Circulation*, 94, II32-7 (1996)
28. Pham, C. T., D. M. MacIvor, B. A. Hug, J. W. Heusel & T. J. Ley: Long-range disruption of gene expression by a selectable marker cassette. *Proc Natl Acad Sci U S A*, 93, 13090-5 (1996)
29. Johnson, P. & T. Friedmann: Limited bidirectional activity of two housekeeping gene promoters: human HPRT and PGK. *Gene*, 88, 207-13 (1990)
30. Scacheri, P. C., J. S. Crabtree, E. A. Novotny, L. Garrett-Beal, A. Chen, K. A. Edgemon, S. J. Marx, A. M. Spiegel, S. C. Chandrasekharappa & F. S. Collins: Bidirectional transcriptional activity of PGK-neomycin and unexpected embryonic lethality in heterozygote chimeric knockout mice. *Genesis*, 30, 259-63 (2001)
31. Nesterova, T. B., C. M. Johnston, R. Appanah, A. E. Newall, J. Godwin, M. Alexiou & N. Brockdorff: Skewing X chromosome choice by modulating sense transcription across the Xist locus. *Genes Dev*, 17, 2177-90 (2003)
32. Jerome, L. A. & V. E. Papaioannou: DiGeorge syndrome phenotype in mice mutant for the T-box gene, Tbx1. *Nat Genet*, 27, 286-91 (2001)

33. Cousley, R., H. Naora, M. Yokoyama, M. Kimura & H. Otani: Validity of the Hfm transgenic mouse as a model for hemifacial microsomia. *Cleft Palate Craniofac J*, 39, 81-92 (2002)
34. Naora, H., M. Kimura, H. Otani, M. Yokoyama, T. Koizumi, M. Katsuki & O. Tanaka: Transgenic mouse model of hemifacial microsomia: cloning and characterization of insertional mutation region on chromosome 10. *Genomics*, 23, 515-9 (1994)
35. Le Douarin, N. M.: Developmental and Cell Biology Series. Cambridge Univ. Press, Cambridge (1982)
36. Morrison, P. J., H. C. Mulholland, B. G. Craig & N. C. Nevin: Cardiovascular abnormalities in the oculo-auriculo-vertebral spectrum (Goldenhar syndrome). *Am J Med Genet*, 44, 425-8 (1992)
37. Araneta, M. R., C. A. Moore, R. S. Olney, L. D. Edmonds, J. A. Karcher, C. McDonough, K. M. Hiliopoulos, K. M. Schlangen & G. C. Gray: Goldenhar syndrome among infants born in military hospitals to Gulf War veterans. *Teratology*, 56, 244-51 (1997)
38. Kenneth Lyons Jones, M.: Smith's Recognizable Patterns of Human Malformation, 5th. WB Saunders Co, Philadelphia (1997)
39. Lin, H. J., T. R. Owens, R. M. Sinow, P. C. Fu, Jr., A. DeVito, M. H. Beall & R. S. Lachman: Anomalous inferior and superior venae cavae with oculoauriculovertebral defect: review of Goldenhar complex and malformations of left-right asymmetry. *Am J Med Genet*, 75, 88-94 (1998)
40. Kanagasuntheram, R. & J. A. Verzin: Ectopia cordis in man. *Thorax*, 17, 159-67 (1962)

Key Words: Zic3, over-expression, kyphosis, hemifacial microsomia, ectopia cordis, Goldenhar Syndrome

Send correspondence to: John W. Belmont, M.D.,Ph.D., Department of Molecular and Human Genetics, Baylor College of Medicine, One Baylor Plaza, Houston, TX 77030 Tel: 713-798-4634, Fax: 713-798-8142, E-mail: jbelmont@bcm.tmc.edu

http://www.bioscience.org/current/vol12.htm